Earthq Sci (2014) 27(1):37–46
DOI 10.1007/s11589-013-0048-6

RESEARCH PAPER

Failure time variation derived from R–S relation: the role of the static stress perturbation

Qiu Zhong · Wenhao Shen · Baoping Shi

Received: 2 September 2013 / Accepted: 26 November 2013 / Published online: 18 December 2013

Abstract In general, earthquake cycle related to earthquake faulting could include four major processes which could be described by (1) fault locking, (2) self-acceleration or nucleation (possible foreshocks), (3) coseismic slip, and (4) post-stress relaxation and afterslip. A sudden static stress change/perturbation in the surrounding crust can advance/delay the fault instability or failure time and modify earthquake rates. Based on a simple one-dimensional spring-slider block model with the combination of rate-and-state-dependent friction relation, in this study, we have approximately derived the simple analytical solutions of clock advance/delay of fault failures caused by a sudden static *Coulomb* stress change applied in the different temporal evolution periods during an earthquake faulting. The results have been used in the physics-based explanation of delayed characteristic earthquake in Parkfield region, California, in which the next characteristic earthquake of *M* 6.0 after 1966 occurred in 2004 instead of around 1988 according to its characteristic return period of 22 years. At the same time, the analytical solutions also indicate that the time advance/delay in *Coulomb* stress change derived by the dislocation model has a certain limitation and fundamental flaw. Furthermore, we discussed the essential difference between rate- and state-variable constitutive (R–S) model and *Coulomb* stress model used commonly in current earthquake triggering study, and demonstrated that, in fact, the *Coulomb* stress model could be involved in the R–S model. The results, we have obtained in this study, could be used in the development of time-dependent fault interaction model and the probability calculation related to the time-dependent and renewal earthquake prediction model.

Keywords Earthquake triggering · Fault friction · *Coulomb* stress change (ΔCFF) · Clock advance/delay · Rate-and-state-dependent friction

Q. Zhong (✉) · W. Shen · B. Shi
University of Chinese Academy of Sciences, Beijing 100049, China
e-mail: zhongqiu09@mails.ucas.ac.cn

1 Introduction

Parkfield lies along the San Andreas Fault, one of the longest and most active faults in the United States. The 40-km-long Parkfield section of the San Andreas Fault was recognized two decades ago as a promising earthquake physics laboratory, and an intensive experiment was established to record the next segment-rupturing earthquake there and provide the much-needed detailed observations (Bakun et al. 2005). Moderate-size earthquakes of about magnitude 6 have occurred on the Parkfield section of the San Andreas fault at fairly regular intervals—in 1857, 1881, 1901, 1922, 1934, and 1966 (Figs. 1, 2). While little is known about the first three shocks, available data suggest that all six earthquakes may have been "characteristic" in the sense that they occurred with some regularity (mean repetition time of about 22 year) and may have repeatedly ruptured the same area on the fault (Bakun and Lindh 1985; Bakun and McEvilly 1979). The times between sequences since 1857 are remarkably uniform, with a mean interval of about 22 years. The similarity of waveforms recorded in the 1922, 1934, and 1966 events is possible only if the ruptured area of the fault is virtually the same for all three events (Bakun et al. 2005). The *M*6 critical earthquakes in Parkfield provide an opportunity for scientists to better understand the physics of earthquakes—what actually happens on the fault and in the surrounding region before, during, and after an earthquake.

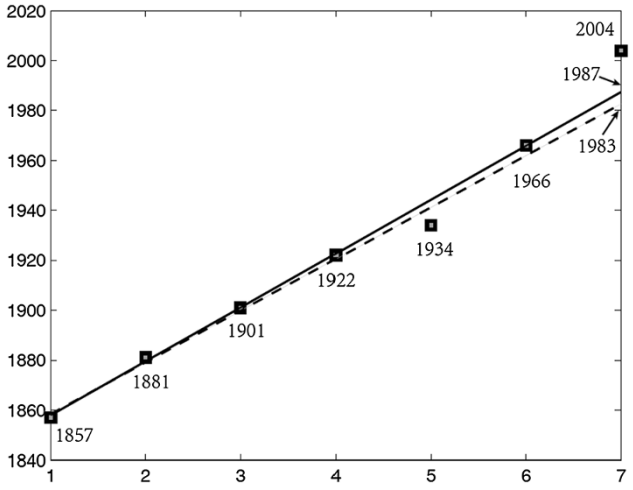

Fig. 1 *M*6.0, the significant earthquakes have occurred on the Parkfield section of the San Andreas fault at fairly regular intervals—in 1857, 1881, 1901, 1922, 1934, and 1966. The next significant earthquake was anticipated to take place within the time frame 1988–1993. *Solid line* is a linear fit without the 1934 event, and *dashed line* includes it

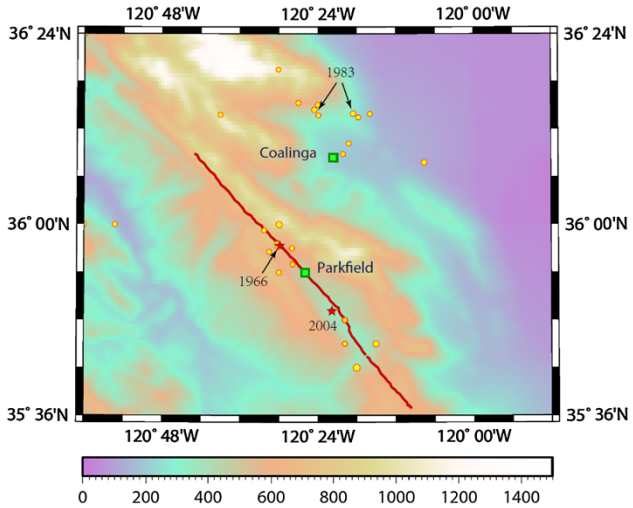

Fig. 2 Location of $M > 5$ earthquakes in and around Parkfield from 1857 to 2005 (*yellow circles*). The *red line* represents the San Andreas fault. *Red stars* are respectively 1966 and 2004 characteristic earthquakes on the fault. In 1983, the *M*6.5 *Coalinga* and *M*6.0 *Nuñez* events struck 25 km northeast of Parkfield. *Arrows* shows the two largest earthquakes

By studying the faulting mechanism, magnitude, rupture length, location, and other some cases of five *M*6 earthquake before 1966, Bakun and Lindh (1985) inferred that the average repeat time of the characteristic earthquakes in Parkfield is 22 years and proposed that the next earthquake after the 1966 *M*6.0 earthquake occurred in 1985–1993. However, it did not occur until September 28, 2004. The similar amplitudes and waveforms of 1922, 1934, 1966, and 2004 earthquakes imply the same seismic moment, focal mechanism, and teleseismic wave path (Bakun et al. 2005). Many scholars from different perspectives give explanations on clock delay of the 2004 Parkfield *M*6.0 earthquake. Ben-Zion et al. (1993) proposed that interaction effects due to the distant *M*7.9 1906 and nearby *M*7.9 1857 earthquakes have modulated the timing of *M*6.0 Parkfield earthquakes. Toda and Stein (2002) studied the response of the San Andreas Fault to the 1983 *Coalinga-Nuñez* earthquakes, and supposed that 1983 shocks dropped the 10-year probability of a *M*6 Parkfield earthquake by 22 %, which explains why the Parkfield earthquake did not strike in the 1980s, but not why it was absent in the 1990s. Barbot et al. (2012) developed an integrative and fully dynamic model of the Parkfield segment of the San Andreas Fault, giving recurrence time between 15 and 25 years, and indicated that the delay of the latest M_w6.0 2004 event at Parkfield and its unexpected change of hypocenter may have been at least partially caused by the smaller earthquakes in 1992–1994, a series of arrested M_w6.0 nucleations.

How to accurately obtain the time of occurrence of the earthquake is one of the most important and fundamental goals in earthquake science with associated earthquake prediction. However, the exploration is still in an elusive stage. Nevertheless, the studies of aftershock triggering mechanism related to its spatial–temporal evolution have made a lot of progress. For this reason, the earthquake triggering mechanism got a lot of attention during recent two decades (Freed 2005). Recent studies indicate that earthquake can be triggered both in terms of near-field (<2–3 fault length) and the far-field. Its mechanism generally can be divided into static stress triggering and dynamic stress triggering, respectively. Many of these studies show a positive correlation between the spatial distributions of aftershocks, or sequences of moderate to large events, with modeled changes in static Coulomb failure stresses generated by earlier nearby large earthquakes (Gomberg et al. 1998; Stein et al. 1997; Harris and Simpson 1998). Static stress change calculations have also provided a good explanation for seismicity rate increases and decreases that occur well outside the above defined aftershock zone (Parsons 2002). Dynamically triggered earthquakes might also make up an important percentage of earthquakes associated with calculated static stress increases, particularly those that happen shortly after the main shock. Discussion of the trigger on static or dynamic trigger mechanism is still an important subject of current academic research.

Calculation of static Coulomb stress change after the mainshock (King et al. 1994) has become an effective tool for quantitative description of aftershock activity. Positive Coulomb stress changes generally correspond to a significant increase in seismic activity; otherwise, negative

Coulomb stress changes generally correspond to a seismic activity decline and form a so-called seismic shadow zone. The calculation of the Coulomb stress change can give the most critical parameter of the time-dependent and renewal earthquake forecasting model (Harris 1998; Toda and Stein 2002). There are several forms of rate- and state-variable (R–S) constitutive law have been widely used to model laboratory observations of rock friction (Scholz 1998). Based on the R–S constitutive law and one-dimensional spring-slider block model, Dieterich (1994) established a theoretical model of aftershock triggering mechanism. The theory has been used to describe the quantification of the *Omori*'s law. In this article, starting from the R–S constitutive law, we investigate clock advance or delay of an earthquake related to static Coulomb stress change on the fault and compare it with Coulomb model of elastic dislocation theory. Furthermore, we attempt to apply research result in this paper to the *M*6 earthquakes in Parkfield, California, USA.

2 *Coulomb* model in elastic dislocation theory

In the *Coulomb* stress change model, the instability moment of a single fault will advance or delay by the static *Coulomb* stress change *Coulomb* Failure Function (ΔCFF). It is generally called the clock advance/delay. Under the elastic dislocation theory, clock advance/delay Δt_{ED} is related to the *Coulomb* stress change by

$$\Delta t_{\mathrm{ED}} = \frac{\Delta \mathrm{CFF}}{\dot{\tau}} = \frac{\Delta\tau - \bar{\mu}\Delta\sigma}{\dot{\tau}}, \tag{1}$$

where $\Delta\tau$ and $\Delta\sigma$ are respectively the shear stress perturbation and the effective normal stress perturbation on the fault, $\bar{\mu}$ is the effective *Coulomb* friction coefficient, $\dot{\tau}$ represents a constant shear stressing rate in the far-field. Equation (1) is widely applied in the explanation of the causes of the seismic shadow zone and the calculation of the time-dependent of earthquake probabilities (Harris 1998; Toda et al. 1998; Parsons et al. 2000).

As we know, although the Coulomb stress changes in the elastic dislocation theory model have been successfully used in many of the simulation of earthquake sequences (King et al. 1994; Stein et al. 1997; Toda and Stein 2002), its limitations are also obvious: The process of fault instability caused by Coulomb stress change obeys the simple friction kinematics, which implied slip weakening conditions of the time predictable model. Figure 3 shows the clock advance/delay of fault failure time Δt_{ED} caused by a static Coulomb stress perturbation in Coulomb Stress Change Model. By loading the step function of the Coulomb stress on the fault (see Fig. 3), the stress on the fault simultaneously jumped, a sudden rise or fall of the stress entirely dependent on the Coulomb stress changes. After the perturbation, stress on the fault continues to increase in the background stress. When shear stress on the fault reaches the rupturing critical strength, the instability occurs, and the original seismic cycle changes by Δt_{ED} [Eq. (1)]. Obviously, it is too simple to describe the evolution process of the fault by the Coulomb stress model based on the simple elastic dislocation theory because the complexity of fault frictional motion is ignored. From Fig. 3, we can see that in the vast majority of seismic circle, whenever the perturbation ΔCFF is given, the clock advance/delay is the same. And at the end of seismic circle, if $\Delta\mathrm{CFF} > 0$, triggering becomes instantaneous. This phase begins from $t_1 = T_{\mathrm{r}} - \Delta t_{\mathrm{ED}}$, and the clock advance $\Delta t_{\mathrm{ED}} = T_{\mathrm{r}} - t_1$, where t_1 is the perturbation time(Gomberg et al. 1998).

Actually, the evolution process of a fault is very complex. Experiment result of rock friction shows that the process of fault friction depends on slip rate $\dot{\delta}$ and state variable θ on the fault (Dieterich 1979; Ruina 1983). In the following, based on the R–S constitutive law and spring-slider block model, we will derive the approximately analytical expression of clock advance/delay Δt corresponding to different stage of earthquake cycle and discuss the limitations of the simple *Coulomb* stress change model given by the elastic dislocation theory.

3 Fault stability analysis based on the R–S constitutive law

R–S constitutive law has been widely used in the study of earthquake generation, source nucleation, and depth constraints (Scholz 1998). Based on the R–S constitutive law and the one-dimension spring-slider block model, Dieterich (1994) established an outstanding model to investigate the aftershock triggering mechanism and used it to describe the

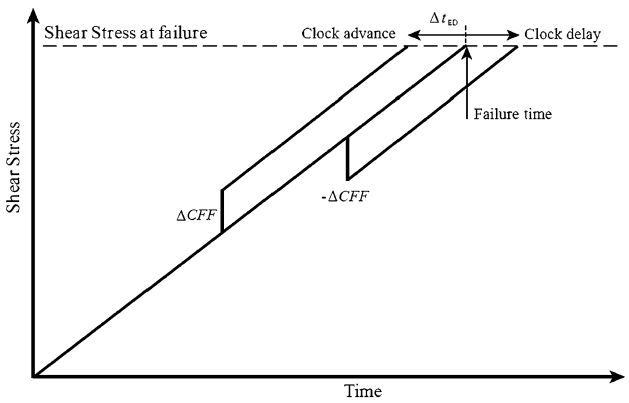

Fig. 3 Clock advance/delay of fault failure time Δt_{ED} caused by a static *Coulomb* stress perturbation in *Coulomb* stress change model

quantification of the Omori aftershock decay process. In Dieterich's (1996) approach, the basic idea comes from the clock advance/delay of an earthquake faulting or earthquake faulting rate change and fault population model (Gomberg 2005) in which each fault with different sizes in the crust is subjected to a sudden static stress perturbation caused by a mainshock. Innovation of this paper is that we focus on the fault evolution changes after the perturbation of the static stress changes at any time within a given seismic circle and attempt to give approximate analytical expressions of the clock advance/delay Δt in each evolutionary stage of the earthquake cycle when subjected to the Coulomb stress perturbations.

3.1 R–S constitutive law

R–S constitutive law provides a basic framework for the quantitative description of the complex properties of the fault frictional motion. Specifically, the rate- and state-variable constitutive law expressed the correlation between the observed instantaneous slip rate and the steady-state slip rate. The rate $\dot{\delta}$ and state θ variable constitutive law of a single fault given by (Dieterich 1979; Ruina 1983):

$$\begin{cases} \tau = \sigma\left[\mu_0 + A\log\left(\dot{\delta}/\dot{\delta}^*\right) + B\log(\theta/\theta^*)\right] \\ \mathrm{d}\theta = \left(1 - \dfrac{\theta\dot{\delta}}{D_c}\right)\mathrm{d}t \end{cases} \tag{2}$$

where τ and σ are shear stress and normal stresses on the fault, respectively, and $\dot{\delta}$ is fault slip rate. The state variable θ is related to time and slip rate. It has the same dimension with time t and specifically descries the aging process on the fault. Parameters μ_0, A, and B are experimentally determined coefficients. The terms with asterisks are normalizing constants. Expression $A\log\left(\dot{\delta}/\dot{\delta}^*\right)$ is to characterize the viscous resistance in the sliding surface caused by some small deformation of irregular or obstacles body like, and $B\log(\theta/\theta^*)$ represents the chemical adhesion between the two surfaces which is proportional to the contact time. Equation (2) has been widely used in the study of kinematics and dynamics of fault evolution.

3.2 One-dimension spring-slider block model

Consider a simple spring-slider block model with spring stiffness k (Fig. 4), the shear stress on the fault τ is given by

$$\tau = \tau_0 - k[\delta(t) - \delta_0(t)], \tag{3}$$

where $\delta_0(t)$ is far-field slip displacement, and the stiffness $k = G\eta/l$ (Dieterich 1992, 1994), G is Shear modulus, and η is the geometrical parameter describing the crack (generally taken to be 1) (Dieterich 1986). Fault will be unstable under the condition: $k < k_c = (B - A)\sigma/D_c$ (Scholz 1998), k_c is critical spring stiffness. Parameter τ_0 is initial shear stress on the fault. If the far-field shear slip rate $\dot{\delta}_0(t)$ is constant and nonzero, the shear stressing rate $\dot{\tau} = k\dot{\delta}_0(t)$.

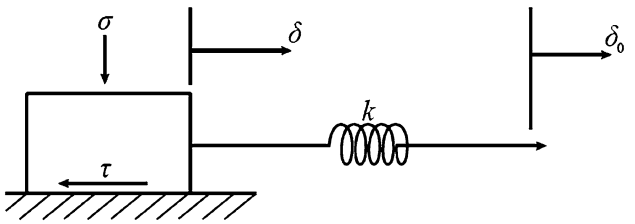

Fig. 4 Spring-slider block model with kinematic equation of motion. τ and σ are the shear stress and normal stress acting on the fault, respectively. δ is the sliding displacement along the fault plane, and δ_0 is a far-field loading displacement. k is the effective elastic coefficient of the spring

In the given initial conditions, when A, B, and D_c are constants, the numerical solution of Eqs. (2) and (3) shows that the evolution of fault slip (seismic circle) can be separated into three distinct phases (Fig. 5). Real evolution of the fault is actually more complex; however, one-dimensional spring-slider block model has visually described the basic process of the fault evolution. The discussion of the above model provides the most basic physical ideas to investigate more deeply into the causes of earthquakes the mechanism.

3.3 Time-dependent deformation process

The instability of the fault is determined by the *Coulomb* stress at the depth which earthquakes may nucleate (Byerlee 1978). The *Coulomb* stress model is given by:

$$\tau - \mu_0\sigma = 0, \tag{4}$$

where, τ is the shear stress amplitude in the slip direction and σ is the effective normal stress on the fault including pore water pressure. In the given back ground stress field τ_1 and σ_1, when there is a shear stress change $\Delta\tau$ and normal stress change $\Delta\sigma$ from the coseismic process or other non-tectonic stress change, the new stress field is expressed as: $\tau_2 = \tau_1 + \Delta\tau$, $\sigma_2 = \sigma_1 + \Delta\sigma$. Furthermore, we assume that all the stress perturbation $\Delta\tau \ll \tau_1$, $\Delta\sigma \ll \sigma_1$, the *Coulomb* stress change thus be written as: $\Delta\mathrm{CFF} = \Delta\tau - \mu_0\Delta\sigma$ (ΔCFF). According to Eqs. (2) and (4), the fault slip rate on the fault after the stress perturbation $\dot{\delta}_2$ could be calculated as follows:

$$\dot{\delta}_2 = \dot{\delta}_1\left(\frac{\theta_2}{\theta_1}\right)^{-\frac{B}{A}}\exp\left(\frac{\Delta\mathrm{CFF}}{A\sigma_2}\right), \tag{5}$$

where $\dot{\delta}_1$. is the slip rate on the fault before the stress perturbation, θ_1 and θ_2 reflect the changes of the contact

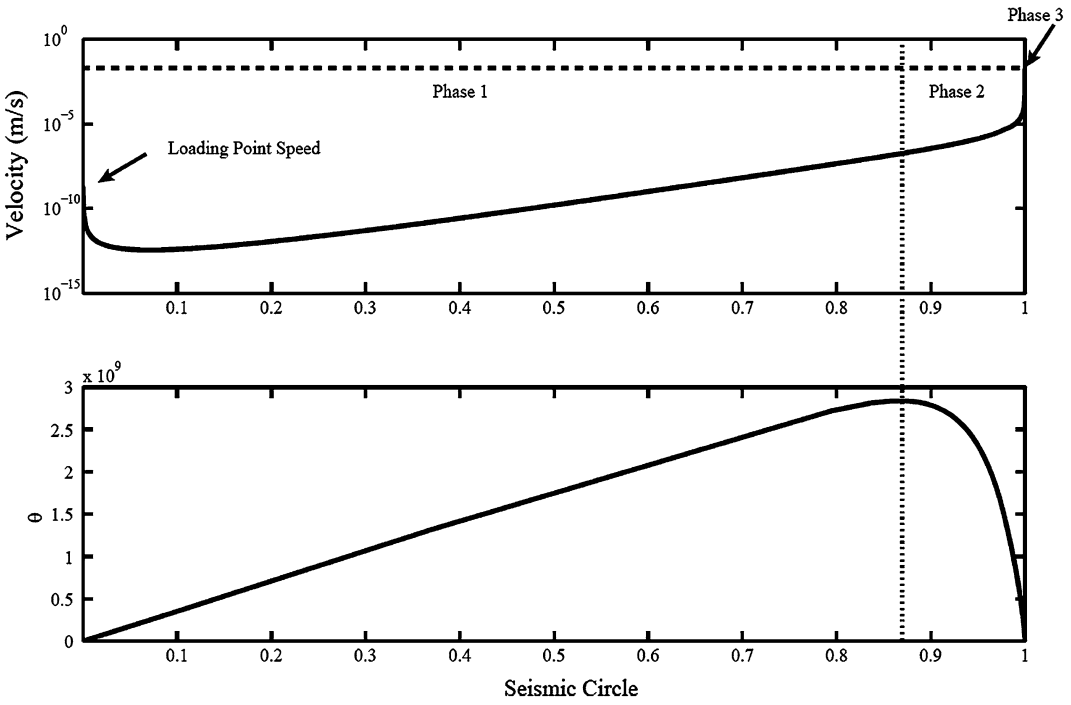

Fig. 5 A typical seismic cycle derived from Eq. (2) (Ziv and Rubin 2003). Fault slip rate δ (*top plot*) and state θ (*bottom plot*) vary with time throughout an entire seismic cycle. In "*Phase 1*", the fault is approximated locked, and slip rate is well below that of the loading point. In "*Phase 2*", the fault slip rate increases rapidly. "*Phase 3*" represents the co-seismic rupture. Correspondingly, fault state variable θ increases linearly in "*Phase 1*" reaching to maximum value in which $\mathrm{d}\theta/\mathrm{d}t = 0$ and decreases rapidly in "*Phase 2*", then back to the initial value of the seismic cycle in "*Phase 3*"

status on the fault before and after the stress perturbation. Equation (5) can also be written in a logarithmic form:

$$\Delta \log\left(\dot{\delta}\right) = -\frac{B}{A}\Delta \log(\theta) + \frac{\Delta \mathrm{CFF}}{A\sigma_2} \tag{6}$$

Constants of A and B typically have values in the range 0.005–0.010 (Dieterich 1992). Ratio of B/A expressed the different mechanisms of fault friction process. $B > A$ Corresponds to the velocity weakening behavior, and $B < A$ is velocity strengthening, which is intrinsically stable, and no earthquake can nucleate in this field, and any earthquake propagating into this field will produce there a negative stress drop, which will rapidly terminate propagation (Scholz 1998). Figure 5 shows that according to Eq. (2), Ziv and Rubin (2003) separate the seismic cycle into three distinct phases. However, in this research, according to changes of the state rate and slip rate, we separate the seismic cycle into three major different stages. 1. In stage 1, fault is nearly locked, the sliding velocity is much less than 1, $\dot{\delta} \ll 1$. The rate of state, thus, may be written as $\mathrm{d}\theta/\mathrm{d}t \sim 1$ (Beeler et al. 1994). And the evolution of slip rate may be given by $\dot{\delta}_2 \sim \dot{\delta}_1$. 2. Stage 2 has a very short time. When the fault convert from "phase 1" locked state to "phase 2" self-acceleration, there is $\mathrm{d}\theta/\mathrm{d}t \sim 0$; 3. Stage 3, the rate of state and the slip velocity are given by $\mathrm{d}\theta/\mathrm{d}t \sim -\dot{\delta}\theta/D_\mathrm{c}$ and $\dot{\delta} \gg D_\mathrm{c}D_\mathrm{c}/\theta$, respectively.

3.4 Calculation of Δt in each evolutionary stage

Parameter $\dot{\delta}_0$ in Fig. 6 means the slip rate on the fault at the moment t_0 (the initial time of seismic cycle); $\dot{\delta}_1$ and $\dot{\delta}_2$ are the fault slip rates at times of t_1 and t_2, respectively. Stress perturbation applied on the fault starts at time of t_1, and Δt is the advance/delay time caused by the stress change on the fault. T_r is the mean earthquake recurrence time of a seismogenic fault; T_1 is the time period between t_1 and the failure time before stress perturbation; T_2 is the time period between t_1 and the failure time after stress perturbation.

The figure above (Fig. 6) shows the clock advance/delay caused by a sudden static stress perturbation. The slip rate changes significantly by the stress perturbations, which makes the final rupture time advanced. Starting from the Eq. (6), we specifically analyze the clock advance/delay by static stress perturbations in each evolution stage:

1. When $\mathrm{d}\theta/\mathrm{d}t = 1$ and $\dot{\delta}_2 \sim \dot{\delta}_1$, $\Delta \log\left(\dot{\delta}\right) \sim 0$, Eq. (6) becomes

$$\frac{\Delta\theta}{\theta_1} = \frac{A}{B}\frac{\Delta \mathrm{CFF}}{A\sigma_2} \tag{7}$$

and $\mathrm{d}\theta/\mathrm{d}t = 1$ gives $\Delta\theta = \Delta t$, $\theta_1 = t_1$. Thus, the clock advance/delay is given by

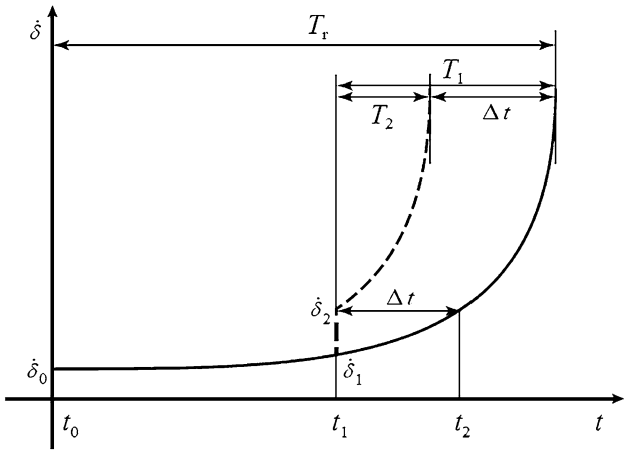

Fig. 6 Schematics showing the clock advance/delay based on the R–S law

$$\Delta t = t_1 \frac{A}{B} \frac{\Delta \mathrm{CFF}}{A\sigma_2} \tag{8}$$

Equation (8) shows that when fault is almost locked in stage, Δt, the clock advance/delay is proportional to *Coulomb* stress change ΔCFF and inversely proportional to normal stress on the fault σ. And note that Δt is proportional to state variable θ. According to $t_a = A\sigma/\dot{\tau}$ (Dieterich 1994), Eq. (8) can be written as

$$\Delta t = \frac{t_1}{t_a} \frac{A}{B} \frac{\Delta \mathrm{CFF}}{\dot{\tau}} \tag{9}$$

Actually, in the study of brittle failure (Beeler 2004), the time period of self-acceleration phase is equal to the aftershocks duration after the main shock t_a (Dieterich 1994). When the average recurrence interval of a single fault T_r is given, the aftershock duration is $t_a = T_r A\sigma/\Delta\tau$, where the average stress drop $\Delta\tau = 1$–10 MPa, which does not depend on the magnitude of earthquake. And if $A\sigma = 0.1$ MPa (Belardinelli 1999),

$$t_a = (1\% - 10\%)T_r \tag{10}$$

Equation (10) gives the probability that the clock advance/delay Δt may rise up to several times to tens of clock advance/delay Δt_{ED} given in the elastic dislocation theory [Eq. (1)] as we mentioned above.

2. When $\mathrm{d}\theta/\mathrm{d}t = 0$, the state variable θ is a constant. From Eqs. (2) and (3), the shear stress can be written as

$$\sigma\left[\mu_0 + A\,\log\left(\dot{\delta}/\dot{\delta}^*\right) + B\,\log(\theta/\theta^*)\right] = \tau_0 + \dot{\tau}t - k\delta(t) \tag{11}$$

where δ, the slip displacement on the fault, can be approximately seen as a constant. The clock advance/delay Δt is computed by taking the time derivation of Eq. (11) and writing in a differential form:

$$A\sigma\Delta\log\dot{\delta} = \dot{\tau}\Delta t, \tag{12}$$

Compare Eqs. (6) and (12), clock advance/delay is given by

$$\Delta t = \frac{\Delta \mathrm{CFF}}{\dot{\tau}}, \tag{13}$$

Equation (13) has the same expression as the clock advance/delay Δt_{ED} given by the simple elastic dislocation theory (Eq. 1).

3. When $\mathrm{d}\theta/\mathrm{d}t = -\dot{\delta}\theta/D_c$, the solution of the state equation is (Dieterich 1994):

$$\theta(t) = \theta_0 \exp\left(-\frac{\delta(t)}{D_c}\right), \tag{14}$$

According to Taylor series, the expression of $\delta(t)$ at t_1 is $\delta(t) = \delta_1 + \dot{\delta}_1\Delta t$. From Eqs. (6) and (14), the differential form of logarithmic slip rate is given by

$$\Delta\,\log\left(\dot{\delta}\right) = \frac{B}{A}\frac{\delta_1 + \dot{\delta}_1\Delta t_1}{D_c} + \frac{\Delta \mathrm{CFF}}{A\sigma}, \tag{15}$$

when the stress perturbation is zero (undisturbed), Eq. (15) can be written as

$$\Delta\,\log\left(\dot{\delta}\right) = \frac{B}{A}\frac{\delta_1 + \dot{\delta}_1\Delta t_0}{D_c} \tag{16}$$

Subtract Eqs. (15) and (16), we can get the clock advance/delay in self-acceleration stage

$$\Delta t = \Delta t_0 - \Delta t_1 = \frac{A}{B}\frac{\Delta \mathrm{CFF}}{A\sigma}\frac{D_c}{\dot{\delta}_1} \tag{17}$$

In fact, Eq. (17) is the approximate solution of the Dieterich's formulation of clock advance/delay (see Appendix), which shows that Δt is proportional to the critical slip displacement D_c and inversely proportional to the slip rate. In Eq. (17), if we assume that $A/B = 1$, $A\sigma = 0.4 \times 10^5$ Pa (Toda and Stein 2002), $D_c = 1$–2×10^{-2} m, when earthquake happens the slip rate $\dot{\delta} = 1$ m/s, the obtained clock advance/delay $\Delta t \sim 0$. Furthermore, if a static Coulomb stress change of $\Delta\mathrm{CFF} = 0.5 \times 10^5$ Pa is applied the Park field fault segment, and the fault slip rate of $\dot{\delta}_0$ is about 2.3×10^{-2} m/a, then, the calculated $\Delta t = 0.5$–1a.

4 Application on the Parkfield *M*6 earthquakes

May 2, 1983, the *M*6.5 earthquake occurred 25 km northeast of Parkfield in *Coalinga*. After that *Nuñez* took place more than one *M*6 earthquakes on 11 June to 22 July in the same year (Fig. 2). The 1983 *Coalinga–Nuñez* earthquakes occurred 17 years after the 1966 Parkfield characteristic earthquake, and seismicity rates climbed for 18 months

along the creeping section of the San Andreas north of Parkfield (Toda and Stein 2002). In order to simplify the parameter selection, we have just considered about the Parkfield section. And the Parkfield characteristic earthquakes have a mean repetition time of about 22 years. According to Eq. (9), the aftershock duration t_a is about 0.2–2 years. Toda and Stein (2002) studying the Parkfield earthquake probabilities to find the duration of the Parkfield aftershock duration t_a that is approximately 1–4 years. In the study of physical basis of brittle failure and their implications for earthquake occurrence and earthquake nucleation, Beeler (2004) pointed out that the aftershock duration t_a (Dieterich 1994) is equal to the time period of self-acceleration phase in seismic circle. Therefore, the 1983 *Coalinga–Nuñez* earthquakes happened in the first stage (Fig. 5) of the seismic circle of the Parkfield characteristic earthquake after 1966 earthquake, and the clock advance/delay Δt is determined by Eq. (8). After the *Coalinga–Nuñez* earthquakes, the *Coulomb* stress drops by about -0.15×10^5 Pa in the Parkfield region (Toda and Stein 2002). Each stress perturbation causes change of fault evolution, which means the clock advance/delay caused by the second stress perturbation should be calculated at the new state after the first stress perturbation. Thus, when a single fault is disturbed by several earthquakes at the evolution stage "Phase 1", the clock advance/delay Δt_i of each stress change $\Delta \mathrm{CFF}_i$ can be written as

$$\Delta t_i = \left(t_{i-1} + \sum_{i=2}^{n} \Delta t_{i-1} \right) \frac{A}{B} \frac{\Delta \mathrm{CFF}_i}{A\sigma} \tag{18}$$

We take the May 2 *M*6.5 earthquake and July 22 *M*6.0 earthquake as the main impact in the Parkfield area. Stress drop is regarded to be invariant in a seismic region (Junn et al. 2002), thus, we consider the *Coulomb* stress drop by the two earthquakes are both 0.075×10^5 Pa. When $t_a = 2$–4a and the corresponding $A\sigma = 0.2$–0.4×10^5 Pa (Toda and Stein 2002), the clock advance/delay caused by *Coalinga–Nuñez* earthquakes is

$$\Delta t_1 = t_1 \frac{A}{B} \frac{\Delta \mathrm{CFF}_1}{A\sigma}, \ \Delta t_2 = (t_1 + \Delta t_1) \frac{A}{B} \frac{\Delta \mathrm{CFF}_2}{A\sigma}, \tag{19}$$

And the total clock advance/delay $\Delta t = \Delta t_1 + \Delta t_2$ is about 16 years ($A\sigma = 0.2$) $\sim$8 years ($A\sigma = 0.4$). In the calculation, we assumed that the fault constitutive parameters A and B are almost equal. In the velocity weakening model, the actual clock advance/delay Δt should be a little smaller than the calculated results, for the fault constitutive parameters $A \leq B$. And the result of clock advance/delay is inversely proportional to the value of $A\sigma$ which is ranges between 0.01 and 0.1 MPa from previous researches (e.g., Belardinelli 1999; Dieterich 1994; Harris and Simpson 1998; Toda and Stein 2002). And the value can be calculated from aftershock duration t_a and shear stressing rate: $A\sigma = \dot{\tau} t_a = \Delta\tau t_a / T_r$. Although there are errors in the final result which caused by the error of parameters, the results show that when the fault at the first stage of seismic circle clock advance/delay affect by a small *Coulomb* stress change can be significant. However, if we use the *Coulomb* model under the elastic dislocation theory $\Delta t_{\mathrm{ED}} = \Delta \mathrm{CFF}/\dot{\tau}$ (King et al. 1994; Stein et al. 1997), the clock advance/delay is proportional to the *Coulomb* stress change, which means the clock delay of the Parkfield characteristic earthquake after 1966 is only about 1.5 years. And approximate solution of Dieterich's formulation corresponds to the self-acceleration stage, Eq. (17) shows that the clock advance/delay is smaller than which calculated by the *Coulomb* stress model under the elastic dislocation theory. Applied in the Parkfield area, the clock advance/delay years $\Delta t < 1.5$. Toda and Stein (2002) supposed that the 1983 shocks dropped the 10-year probability of a *M*6 Parkfield earthquake by 22 % and that the probability did not recover until about 1991. Table 1 gives the clock delay of the Parkfield characteristic earthquake after 1966.

5 Discussion

Although the Eq. (1) is widely used in the interpretation of the seismic shadow zone and time-dependent of earthquake probabilities (Harris 1998; Toda et al. 1998; Parsons et al. 2000), the limitation is obvious. If the evolution of fault is given by R–S constitutive law, then the expression of clock advance/delay based on *Coulomb* stress model in the elastic dislocation theory corresponds to $\mathrm{d}\theta/\mathrm{d}t = 0$, which means the state variable θ in R–S constitutive law is a constant; the friction process is independent of state evolution on the fault. Since the fault sliding nearly constant, the shear stress loading on the fault is linear and mainly related to the far-field shear stress loading rate.

Actually, the process of fault instability in the *Coulomb* stress model according to the simple friction kinematics, which implied a prediction model under the velocity weakening, that is, the evolution process of the fault has nothing to do with the clock advance/delay Δt, which only change with the size of stress perturbation. We can see that the *Coulomb* model based on the R–S constitutive law and which based on the elastic dislocation theory follows the different physical processes. Obviously, the clock advance/delay Δt affected by a given stress perturbation varies at different periods of fault evolution: The clock advance/delay $\Delta t_{\mathrm{RSF}} > \Delta t_{\mathrm{ED}}$ in the most part of the evolution stage 1, $\Delta t_{\mathrm{RSF}} < \Delta t_{\mathrm{ED}}$ in stage 3, and in stage 2, around $t = T_r - t_a$, clock advance/delay $\Delta t_{\mathrm{RSF}} = \Delta t_{\mathrm{ED}}$; Moreover,

Table 1 Clock delay of the Parkfield characteristic earthquake after 1966

Method	Stress drop ($\times 10^5$ Pa)	t_a (a)	Δt (a)
Coulomb model based on the R–S constitutive law			
$d\theta/dt = 1$		2–4	16–8
$d\theta/dt = 0$	0.15	2–4	1.5
$d\theta/dt = -\dot{\delta}\theta/D_c$		2–4	<1.5
Coulomb model under the elastic dislocation theory	0.15		1.5
Toda and Stein (2002)	0.15		Probability did not recover until about 1991

our results are substantially consistent with or close to the numerical rate-state model given by Gomberg et al. (1998; Fig. 5), which means that the clock advance/delay Δt based on the R–S constitutive law given cannot simply expressed by the Eq. (1). Nowadays, the time-dependent and renewal earthquake prediction model is basically built on the understanding of Eq. (1). However, recent studies show that (Gomberg et al. 2005; Kaneko 2009), from Eq. (1), we can deduce that ratio of the seismicity rate in Dieterich's (1994) aftershocks model before and after the main shock is equal to 1. It implies that the *Coulomb* model on the elastic dislocation theory cannot reflect the variation of seismicity rate, as well as the time for fault failure, at least from a mathematical model.

In this research, the clock delay of the *M*6.0 Parkfield earthquake after 1966 is given about 8–16 years. The uncertainty of parameters we used such as aftershock duration t_a and shear stressing rate $\dot{\tau}$ may bring errors to our result. In addition, the other mechanisms, such as fault creeping and post-seismic slip, in the nearby regions of Parkfield could further modify the fault evolution process and contribute to an extra time delay related to the earthquake recurrence period for the *M*6.0 Parkfield fault.

6 Conclusions

Combined with 1D spring-slider block model, we focused our study on the fault failure time advance/delay due to the static *Coulomb* stress perturbation during an entire period of the earthquake fault evolution based on the R–S frictional constitutive relation. We have derived three different analytical expressions of clock advance/delay Δt related to the *Coulomb* stress perturbations applied in the different phase of an earthquake cycle and find that the clock advance/delay Δt is not only affected by the *Coulomb* stress perturbation but also the state variable θ of the fault.

The results, we have derived in this study, also show that the solution given by the *Coulomb* model associated with the elastic dislocation theory has an obvious limitation due to the ignoring of the state variable θ, a function used to describe the fault frictional evolution during a constant stressing rate. When the state variable θ becomes a constant, our solutions of Δt related to the Coulomb stress perturbation are the same as the simple *Coulomb* given by the elastic dislocation theory. In fact, the state variable θ varies at the most part of an earthquake cycle, and the *Dieterich* model [Eq. (24)] can be applied to the self-accelerating stage only. Yet we know that the earthquake faulting is likely to be affected by a stress perturbation in its each evolution stage, and the first stage related to the fault evolution (blocking phase) is actually about 90 % of the whole evolution period. Therefore, the expressions of clock advance/delay under the *Coulomb* stress perturbation we have derived [Eqs. (8), (13), (17)] are much more comprehensive descriptions of the earthquake rate modifications undergoing a sudden change in stress.

Regarding the time delay of recent *M*6.0 Parkfield earthquake after the 1966 *M*6.0 earthquake, we find that, based on current solution, the characteristic earthquake with *M*6.0 after 1966 would delay for 8–16 years when the fault affected by the *Coulomb* stress perturbation $\Delta CFF = -0.15$bar, caused by the 1983 *Coalinga–Nuñez* earthquakes. These results are much more reasonable than that based on the simple *Coulomb* stress model given by the elastic dislocation theory [Eq. (1)].

Finally, our current results could be useful in the establishing of time-dependent earthquake probability model if an earthquake history that is well characterized by paleoseismic or historical observations can be fit with a broad range of interevent time and aperiodicity models.

Appendix: approximate solution of Dieterich's formulation of clock advance/delay

Based on the 1D spring-slider block model described by Fig. 4, when $d\theta/dt = -\dot{\delta}\theta/D_c$ and $\dot{\delta} \gg D_c/\theta$, from Eqs. (2) and (3), the slip rate at t_1 is (Dieterich 1992):

$$\dot{\delta}_1 = \left[\left(\frac{1}{\dot{\delta}_0} + \frac{H\sigma}{\dot{\tau}}\right)\exp\left(-\frac{\dot{\tau}t_1}{A\sigma}\right) - \frac{H\sigma}{\dot{\tau}}\right]^{-1}, \quad (20)$$

where $H = B/D_c - k/\sigma$, $\dot{\delta}_0$, is the initial slip rate.

Change of normal stress from σ_1 to σ_2 results in the change of state $\theta_2/\theta_1 = (\sigma_2/\sigma_1)^{-\alpha/B}$ (Dieterich 1994) although the jumps of shear stress τdo not affect state. In this case, Eq. (5) can be written as

$$\dot{\delta}_2 = \dot{\delta}_1 \left(\frac{\sigma_1 + \Delta\sigma}{\sigma_1}\right)^{\frac{a}{A}} \exp\left(\frac{\Delta \mathrm{CFF}}{A\sigma_2}\right), \tag{21}$$

or given by a differential form:

$$\Delta \log\left(\dot{\delta}\right) = \frac{\Delta\tau - (\mu_0 - \alpha)\Delta\sigma}{A\sigma} = \frac{\Delta \mathrm{CFF}^G}{A\sigma}, \tag{22}$$

Actually, Eq. (22) reflects the relative change of the slip rate following a sudden stress perturbation, and$\Delta \mathrm{CFF}^G = \Delta\tau - (\mu_0 - \alpha)\Delta\sigma$ gives effective shear stress change which can be defined as the generalized *Coulomb* stress disturbance.

If a *Coulomb* stress perturbation as shown in Eq. (22) applied at time t_1, following the Eq. (20), the change of slip rate is given by

$$\begin{aligned}\dot{\delta}_2 &= \dot{\delta}_1 \exp\left(\frac{\Delta \mathrm{CFF}^G}{A\sigma}\right) \\ &= \left[\left(\frac{1}{\dot{\delta}_0} + \frac{H\sigma}{\dot{\tau}}\right)\exp\left(-\frac{\dot{\tau}t_2}{A\sigma}\right) - \frac{H\sigma}{\dot{\tau}}\right]^{-1},\end{aligned} \tag{23}$$

Comparing Eqs. (23) and (20), the clock advance/delay Δt is given by

$$\begin{aligned}\Delta t = &\frac{\Delta \mathrm{CFF}^G}{\dot{\tau}} \\ &- \frac{A\sigma}{\dot{\tau}} \log\left\{1 + \exp\left(-\frac{\dot{\tau}(T_r - t_1)}{A\sigma}\right)\left[\exp\left(\frac{\Delta \mathrm{CFF}^G}{A\sigma}\right) - 1\right]\right\},\end{aligned} \tag{24}$$

where T_r is the average earthquake repeat time (Fig. 6)

$$T_\mathrm{r} = \frac{A\sigma}{\dot{\tau}} \ln\left(\frac{\dot{\tau}}{H\sigma\dot{\delta}_0} + 1\right). \tag{25}$$

Note that Eq. (24) is derived based on the assumption of $\mathrm{d}\theta/\mathrm{d}t = -\dot{\delta}\theta/D_\mathrm{c}$ or $\dot{\delta} \gg D_\mathrm{c}/\theta$. Therefore, this formula only applies to the later period of fault evolution which corresponding to the fault self-acceleration and the source nucleation stage. The nucleation time is shorter in lower effective stress environments. Dieterich (1994) predicts a linear dependence of t_a with normal stress σ as $t_a = A\sigma/\dot{\tau}$, and $\dot{\tau}$ is a constant stressing rate. t_a is also corresponding to the regional aftershock duration when a mainshock occurred. The clock advance/delay Δt given by Eq. (24) is always shorter than Δt_ED given by Eq. (1) based on the simple *Coulomb* stress model. And considering changes of slip state, the model in R–S constitutive law [Eqs. (24), (17)] gives that when $t_1 \to T_\mathrm{r}$ ($\delta_1 \gg D_\mathrm{c}$), clock advance/delay $\Delta t \to 0$.

Furthermore, inserting Eqs. (20) and (25) into Eq. (24), we can get

$$\begin{aligned}\Delta t = &\frac{A\sigma}{\dot{\tau}} \log\left(\frac{\dot{\tau}}{H\sigma\dot{\delta}_1} + 1\right) \\ &- \frac{A\sigma}{\dot{\tau}} \log\left[\frac{\dot{\tau}}{H\sigma\dot{\delta}_1}\exp\left(-\frac{\Delta \mathrm{CFF}^G}{A\sigma}\right) + 1\right] = T_1 - T_2,\end{aligned} \tag{26}$$

where $\dot{\tau}/H\sigma\dot{\delta}_1 = \exp(T_1/t_a) - 1$ and $\exp(-\Delta \mathrm{CFF}^G/A\sigma)\dot{\tau}/H\sigma\dot{\delta}_1 = \exp(T_2/t_a) - 1$,

Under the condition of $\mathrm{d}\theta/\mathrm{d}t = -\dot{\delta}\theta/D_\mathrm{c}$ or $\dot{\delta} \gg D_\mathrm{c}/\theta$, Eq. (26) can be simplified as

$$\Delta t = \frac{A}{H\dot{\delta}_1}\left(1 - \exp\left(-\frac{\Delta \mathrm{CFF}^G}{A\sigma}\right)\right). \tag{27}$$

Furthermore, if $\Delta \mathrm{CFF}^G/A\sigma \ll 1$, with a Taylor's expansion, Eq. (27) can be written as

$$\Delta t = \frac{A}{H\dot{\delta}_1}\frac{\Delta \mathrm{CFF}^G}{A\sigma}\left(1 - \frac{1}{2}\frac{\Delta \mathrm{CFF}^G}{A\sigma}\right), \tag{28}$$

where $H = -k/\sigma + B/D_\mathrm{c}$, $k < k_\mathrm{c} = (B - A)\sigma/D_\mathrm{c}$, (Scholz 1998), giving the relationship that $H > A/D_\mathrm{c}$. A and B generally have the values of 0.005–0.01 (Dieterich 1992), and at the depth of the earthquake nucleation, there is: $B > A$. When the friction falls from the static to the sliding value $k_c D_c = \Delta\tau$ (Dieterich 1978), Eq. (28) can be written as

$$\begin{aligned}\Delta t &= \frac{A}{H\dot{\delta}_1}\frac{\Delta \mathrm{CFF}^G}{A\sigma}\left(1 - \frac{1}{2}\frac{\Delta \mathrm{CFF}^G}{A\sigma}\right) \\ &= \frac{A}{H\dot{\delta}_1}\frac{\Delta \mathrm{CFF}^G}{A\sigma}\frac{A\sigma + k_c D_c - \Delta \mathrm{CFF}^G}{B\sigma} = \frac{A}{B}\frac{\Delta \mathrm{CFF}}{A\sigma}\frac{D_\mathrm{c}}{\dot{\delta}_1},\end{aligned} \tag{29}$$

Equation (29) gives the same the expression as Eq. (17) discussed before when the fault evolution undergoes a self-accelerating or nucleation stages [Eq. (16)].

References

Bakun W, McEvilly T (1979) Earthquakes near Parkfield, California: comparing the 1934 and 1966 sequences. Science 205: 1375–1377

Bakun WH, Lindh AG (1985) The Parkfield California, earthquake prediction experiment. Science 229(4714):619–624

Bakun W, Aagaard B, Dost B, Ellsworth W, Hardebeck J, Harris R, Ji C, Johnston M, Langbein J, Lienkaemper J (2005) Implications for prediction and hazard assessment from the 2004 Parkfield earthquake. Nature 437(7061):969–974

Barbot S, Lapusta N, Avouac J-P (2012) Under the hood of the earthquake machine: toward predictive modeling of the seismic cycle. Science 336:707–710

Beeler N (2004) Review of the physical basis of laboratory-derived relations for brittle failure and their implications for earthquake occurrence and earthquake nucleation. Pure Appl Geophys 161(9):1853–1876

Beeler N, Tullis T, Weeks J (1994) The roles of time and displacement in the evolution effect in rock friction. Geophy Res Lett 21:1987–1990

Belardinelli ME, Cocco M, Coutant O, Cotton F (1999) Redistribution of dynamic stress during coseismic ruptures: evidence for fault interaction and earthquake triggering. J Geophys Res 104(B7):14914–14925

Ben-Zion Y, Rice JR, Dmowska R (1993) Interaction of the San Andreas fault creeping segment with adjacent great rupture zones and earthquake recurrence at Parkfield. J Geophy Res: Solid Earth (1978–2012) 98:2135–2144

Byerlee J (1978) Friction of rocks. Pure Appl Geophys 116(4): 615–626

Dieterich JH (1979) Modeling of rock friction 1. Experimental results and constitutive equations. J Geophy Res 84(B5):2161–2168

Dieterich JH (1992) Earthquake nucleation on faults with rate-and-state-dependent strength. Tectonophysics 211(1–4):115–134

Dieterich J (1994) A constitutive law for rate of earthquake production and its application to earthquake clustering. J Geophy Res 99:2601

Dieterich JHA (1986) Model for the nucleation of earthquake slip. Earthq Source Mech 1986:37–47

Dieterich JH, Kilgore B (1996) Implications of fault constitutive properties for earthquake prediction. Proc Natl Acad Sci 93: 3787–3794

Freed AM (2005) Earthquake triggering by static, dynamic, and postseismic stress transfer. Annu Rev Earth Planet Sci 33:335–367

Gomberg J, Beeler NM, Blanpied ML, Bodin P (1998) Earthquake triggering by transient and static deformations. J Geophys Res 103(B10):24411–24426

Gomberg J, Reasenberg P, Cocco M, Belardinelli ME (2005) A frictional population model of seismicity rate change. J Geophys Res 110(B5):B05S03

Harris RA (1998) Introduction to special section: stress triggers, stress shadows, and implications for seismic hazard. J Geophy Res 103(B10):24324–24347, 24358

Junn JG, Jo ND, Baag CE (2002) Stochastic prediction of ground motions in southern Korea. Geosci J 6(3):203–214

Kaneko Y (2009) Investigations of earthquake source processes based on fault models with variable friction rheology. California Institute of Technology, Pasadena

King GCP, Stein RS, Lin J (1994) Static stress changes and the triggering of earthquakes. Bull Seismol Soc Am 84(3):935–953

Parsons T (2002) Global Omori law decay of triggered earthquakes: large aftershocks outside the classical aftershock zone. J Geophys Res 107(2199):11

Parsons T, Toda S, Stein RS, Barka A, Dieterich JH (2000) Heightened odds of large earthquakes near Istanbul: an interaction-based probability calculation. Science 288(5466):661–665

Ruina A (1983) Slip instability and state variable friction laws. J Geophys Res 88(10):310–359

Scholz CH (1998) Earthquakes and friction laws. Nature 391(6662): 37–42

Stein RS, Barka AA, Dieterich JH (1997) Progressive failure on the North Anatolian fault since 1939 by earthquake stress triggering. Geophys J Int 128(3):594–604

Toda S, Stein RS (2002) Response of the San Andreas fault to the 1983 Coalinga–Nunez earthquakes: an application of interaction-based probabilities for Parkfield. J Geophys Res 107(B6):ESE 6–1–ESE 6–16

Toda S, Stein RS, Reasenberg PA, Dieterich JH, Yoshida A (1998) Stress transferred by the 1995 M_w = 6.9 Kobe, Japan, shock-Effect on aftershocks and future earthquake probabilities. J Geophys Res B10:524–543, 565

Ziv A, Rubin A (2003) Implications of rate-and-state friction for properties of aftershock sequence: quasi-static inherently discrete simulations. J Geophys Res 108(2051):21